

pubs.acs.org/synthbio Letter

Engineering Carboxylic Acid Reductase (CAR) through a Whole-Cell Growth-Coupled NADPH Recycling Strategy

Levi Kramer, Xuan Le, Marisa Rodriguez, Mark A. Wilson, Jiantao Guo, and Wei Niu*

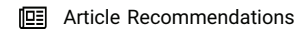


Cite This: ACS Synth. Biol. 2020, 9, 1632-1637



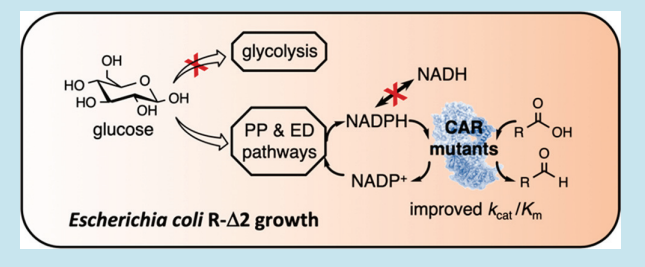
ACCESS

III Metrics & More



Supporting Information

ABSTRACT: Rapid evolution of enzyme activities is often hindered by the lack of efficient and affordable methods to identify beneficial mutants. We report the development of a new growth-coupled selection method for evolving NADPH-consuming enzymes based on the recycling of this redox cofactor. The method relies on a genetically modified *Escherichia coli* strain, which overaccumulates NADPH. This method was applied to the engineering of a carboxylic acid reductase (CAR) for improved catalytic activities on 2-methoxybenzoate and adipate. Mutant enzymes with up to 17-fold improvement in catalytic efficiency



were identified from single-site saturated mutagenesis libraries. Obtained mutants were successfully applied to whole-cell conversions of adipate into 1,6-hexanediol, a C_6 monomer commonly used in polymer industry.

KEYWORDS: carboxylic acid reductase, redox growth coupling, 2-methoxybenzoate, adipate, 1,6-hexanediol, enzyme engineering

arboxylic acid reductase (CAR) catalyzes the NADPHconsuming direct reduction of a carboxylic acid into its corresponding aldehyde through an in situ activation mechanism that is enabled by a post-translationally grafted phosphopantetheinyl group on a serine residue (Figure 1A). 1,2 Over 40 bacterial and fungal CARs have been identified and characterized for in vitro or in vivo syntheses of aldehydes either as end products or as intermediates for subsequent production of alcohols, amines, and hydrocarbons. 3-17 Structural and mechanistic studies of CAR reveal a highly organized catalytic process that is orchestrated by sequentially shuttling substrates through an adenylation (A), a phosphopantetheinylation (P), and a reduction (R) domain. 18-20 The modular structure of CAR enables the application of its individual domains in catalysis and the engineering of hybrid enzymes through domain shuffling. ^{21,22} Due to the broad substrate specificity, CAR can potentially be applied to the syntheses of a wide range of pharmaceutical and industrial chemicals. Meanwhile, CARs often have suboptimal catalytic activities on nonnative substrates, which have prompted large enzyme engineering efforts. ^{23–26} A high-throughput assay was established to quantify the aldehyde products of CARcatalyzed reactions.²⁷ Although the method was successfully applied to the screening of a CAR mutant library of 6×10^3 variants, it is a highly instrument-intensive approach.²³

RESULTS AND DISCUSSION

In order to greatly facilitate CAR engineering efforts, we seek to develop an efficient and affordable method that is based on redox balance, which plays a key role in the survival of cells. Inefficient cycling of redox molecules between oxidized and reduced states results in poor fitness, which can be rescued by the introduction of new redox enzyme(s) to reestablish the balance. Several growth-coupled schemes have been designed and applied to the engineering of redox enzymes and microbial cell factories. $^{28-34}$ Among them, an NADPH auxotrophic E. coli strain was generated as a sensor host for NADPHproducing enzymes.²⁹ Repurposing a metabolic engineering strategy³¹ to elevate intracellular NADPH concentrations through the replacement of an NADH-dependent glycolytic enzyme with NADPH-dependent ones led to an E. coli host that was successfully used for the growth-coupled selection of lactate dehydrogenase mutants with altered cofactor preference for NADPH.30 In this report, we developed an NADPH overaccumulating E. coli strain (Figure 1B), which enabled low-cost and rapid identification of CAR mutants with improved catalytic activities on desired substrates. The strain design entails redirecting the carbon flux of aerobic glucose metabolism from the Embden-Meyerhof-Parnas (EMP) to the oxidative pentose phosphate (PP) and the Entner-Doudoroff (ED) pathways by deleting the *pgi* gene, which encodes glucose 6-phosphate (G6P) isomerase.³⁵ As a result, one NADPH molecule is produced when one G6P molecule is

Received: May 31, 2020 Published: June 26, 2020





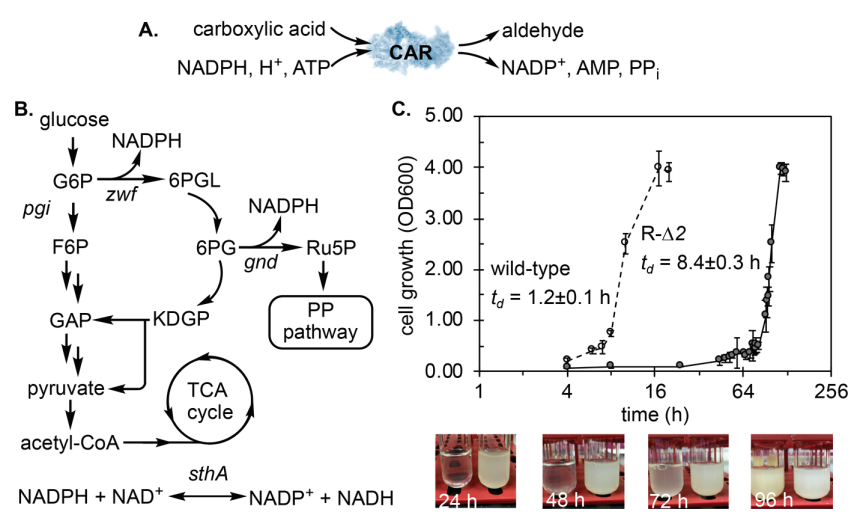


Figure 1. NADPH recycling-based whole-cell growth-coupled strategy for CAR engineering. (A) Reactions catalyzed by CAR enzymes. (B) Schematic representation of an NADPH overaccumulating *E. coli*. Genes encoding the G6P isomerase (pgi) and the soluble transhydrogenase (sthA) are deleted. (C) Growth characterization of *E. coli* strains in liquid minimal media with glucose. (Data are the average of biological triplicates with standard deviations.) Cultures in pictures: right, wild-type, BW25113; left, R- Δ 2, BW25113 Δ pig Δ sthA. Abbreviations: 6PGL, 6-phosphogluconolactone; RuSP, ribulose 5-phosphate; KDGP, 2-keto-3-deoxygluconate 6-phosphate; F6P, fructose 6-phosphate; G3P, glyceraldehyde 3-phosphate.

oxidized by the G6P dehydrogenase (encoded by zwf) (Figure 1B). Furthermore, elevated flux through the PP pathway results in additional NADPH synthesis through the oxidative decarboxylation of 6-phosphogluconate (6PG), which is catalyzed by 6PG dehydrogenase (encoded by gnd, Figure 1B). Since wild-type E. coli is capable of shuttling electrons between NADPH and NADH through activities of transhydrogenases that are encoded by sthA and pntAB, the strain design also included the deletion of the sthA gene, which encodes the soluble transhydrogenase that has the major function of oxidizing NADPH to reduce NAD+.36,37

Establishing Growth-Coupled NADPH-Recycling Se**lection.** An E. coli strain, R- Δ 2, was constructed by deleting both pgi and sthA genes in the K-12 strain BW25113. When cultured in minimal media with glucose as the sole carbon source, R-\Delta 2 showed severe growth retardation with extended lag phase and doubling time (t_d) in comparison to the wildtype strain (Figure 1C). The observed fitness change was hypothesized to be the result of the cell's inability to oxidize excessive NADPH. To verify that cell growth can be rescued by an exogenously introduced NADPH-consuming reaction, the wild-type CAR from Mycobacterium avium (MavCAR) was expressed in R-\Delta2 together with a phosphopantetheinyl transferase (Sfp) from Nocardia iowensis. To minimize metabolic burden caused by high level expression of the MavCAR, the enzyme was expressed from a low copy number vector with pSC101 replication origin and its expression was inducible in the presence of IPTG. The obtained strain was cultured in media with or without benzoate, which is a preferred substrate of MavCAR.¹¹ In the presence of benzoate, a substantially shorter lag phase was observed (Figure 2A). Meanwhile, the cytotoxicity of the compound led to slower growth rate, which was also observed when the wild-type E. coli strain was cultured in the same type of media (Figure S1). A similar trend of cell growth was observed when cells were cultured on agar plates. Colonies of MavCAR-expressing R-Δ2 cells appeared earlier on plates with benzoate (Figure S2). Results from both liquid and solid cultures therefore confirmed

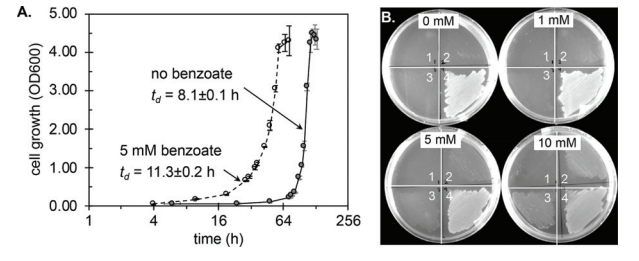


Figure 2. Growth characterization of R- Δ 2 strains expressing MavCAR. (A) In liquid minimal media (1% glucose) without and with benzoate (5 mM). Data are the average of biological triplicates with standard deviations. (B) On solid minimal media (1% glucose) with indicated concentrations of 6-hydroxyhexanoic acid (6-HHA). Plates were incubated at 37 °C for 24 h. Strains were R- Δ 2 expressing Sfp with (1) empty vector, (2) MavCAR, (3) MavCAR-YahK. Strain 4 is wild-type *E. coli.* IPTG at a concentration of 0.25 mM was included in both liquid and solid media.

that CAR-catalyzed reaction recovered the aerobic growth of R- $\Delta 2$ cells on glucose.

Next, we investigated the correlation between the growth rate of R- Δ 2 and the activity level of CAR. To avoid growth difference caused by changes in the expression level of MavCAR, activities of the enzyme in R-Δ2 strain were tuned by culturing cells on minimal media plates containing varied concentrations of 6-hydroxyhexanoic acid (6-HHA), which is not a carbon source and has low cytotoxicity to E. coli (data not shown). Since our previous study showed that MavCAR has a K_m value of 10.0 mM toward 6-HHA,¹¹ we chose to include this compound at concentrations that were equal or lower than the $K_{\rm m}$. After 24 h of incubation, growth of R- $\Delta 2/$ MavCAR strain was observed on plates containing 6-HHA (no. 2 in Figure 2B). Faster growth was observed at higher concentrations. No unambiguous growth was observed for R- $\Delta 2$ transformed with empty vector (no. 1 in Figure 2B). To investigate potential cytotoxicity caused by the aldehyde product of CAR-catalyzed reaction, a broad substrate

specificity aldehyde reductase (YahK) was expressed in R- Δ 2/MavCAR. This addition did not significantly affect the cell growth (no. 3 in Figures 2B). The positive correlation between activities of CAR and the growth of R- Δ 2 strains was further verified using MavCAR and a second CAR from *Mycobacterium marinum* (MmCAR). The two enzymes have different kinetic properties toward 6-HHA but behave similarly on benzoate. Expression of the kinetically better MavCAR led to faster growth in media containing 6-HHA (Figure S3). In the case of benzoate, similar growth rate was observed for cells expressing either CAR (Figure S3). Above results demonstrated that *E. coli* R- Δ 2 is an appropriate host for the detection of CAR variants with improved activities in a protein engineering experiment.

Engineering CAR for 2-Methoxybenzoate Substrate. Our CAR engineering efforts focused on the adenylation step, which is critical for substrate recognition in a CAR-catalyzed reaction. ^{18,22} We built a homology model of the A domain of MavCAR using I-TASSER program³⁸ based on known structures of CAR enzymes with approximate 55% sequence identity (Figure 3A). ¹⁸ An active site consisting of 15 residues

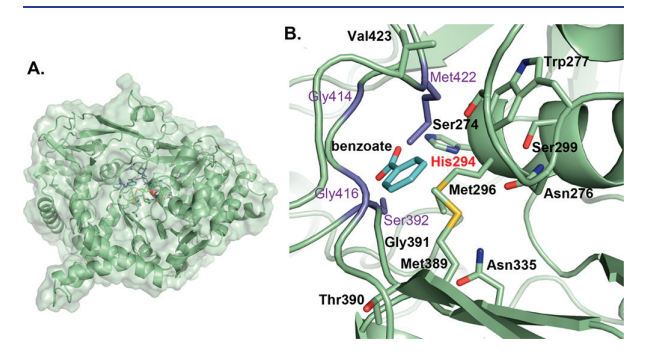


Figure 3. Homology model of the adenylation domain of MavCAR. (A) Overall fold of the A domain. Residues in the active site are shown as sticks. (B) Close-up of the active site. The catalytic His294 is labeled in red. The ten residues that were subjected to engineering are labeled in black. The four residues that were not examined are labeled in purple.

was defined from a docking analysis with benzoate as the substrate using AutoDock Vina³⁹ (Figure 3B). The docking grid box was defined based on the binding mode of benzoate in a known structure of CAR (PDB ID 5MSD). Except for the essential catalytic residue, His294, and four residues that were shown to play insignificant roles in substrate recognition (unpublished data), the remaining ten residues were subjected to single-site saturated mutagenesis using the NNK codon method. Obtained mutant libraries were selected in the R- $\Delta 2$ host expressing Sfp.

The CAR-catalyzed reaction of *ortho*-substituted benzoate was reported to be unfavorable, presumably due to steric hindrance. We therefore chose 2-methoxybenzoate as the first target substrate in CAR engineering. The R- Δ 2 host was transformed with each of the ten libraries. Transformed cells were plated on minimal media plates containing glucose (1%, w/v) and 2-methoxybenzoate (1 mM). Colony formation was monitored and documented every 12 h within a 72 h period. A total of 21 colonies, including 18 with faster growth rate (from N276, M296, S299, N335, and M389 libraries) and three with similar growth rate (from W277 library) to the control, were subjected to DNA sequencing analysis in order to identify

mutations (Table S2). Since one of the three isolates from the W277 library was the wild-type MavCAR, it is an indication of overgrowth during the selection. These three isolates were not further characterized. Five mutants were identified multiple times, one from each library (Table S2). These five multiple-occurrence plus three single-occurrence mutants were expressed, purified to similar purity, and characterized by kinetic assays (Figure S4 and Table 1). All mutants had lower $K_{\rm m}$

Table 1. Kinetic Characterization of MavCAR Variants on 2-Methoxybenzoate $\!\!\!^a$

variants	$K_{\rm m}$ (mM)	$k_{\rm cat}~({\rm min}^{-1})$	$k_{\rm cat}/K_{\rm m}~({\rm min}^{-1}~{\rm mM}^{-1})$
wild-type	2.24 ± 0.08	18.5 ± 0.2	8.3 ± 0.3
N276H (2)	1.14 ± 0.05	27.8 ± 0.3	24.4 ± 1.0
N276L (1)	1.47 ± 0.07	18.8 ± 0.2	12.7 ± 0.6
M296L (3)	1.14 ± 0.04	16.1 ± 0.1	14.2 ± 0.5
S299L (3)	1.84 ± 0.09	29.2 ± 0.4	15.9 ± 0.8
S299W (1)	1.31 ± 0.07	22.9 ± 0.3	17.4 ± 0.9
N335V (2)	0.76 ± 0.04	9.6 ± 0.1	12.6 ± 0.7
N335W (1)	0.55 ± 0.03	21.3 ± 0.3	39.0 ± 2.1
M389W (2)	1.57 ± 0.08	35.8 ± 0.5	22.8 ± 1.2

"Numbers in parentheses represent the occurrence of mutants. Data are the average of three measurements with standard deviations.

values for 2-methoxybenzoate than that of the wild-type enzyme (2.24 mM). The reduction ranged from 20% (S299L) to 4-fold (N335W) (Table 1). Among the five mutants that showed higher $k_{\rm cat}$ values, M389W had an approximate 2-fold increase (Table 1). Meanwhile, mutant N335V had an approximate 50% reduction in $k_{\rm cat}$. Overall, all mutants showed increased catalytic efficiency ($k_{\rm cat}/K_{\rm m}$), while the mutant N335W displayed the highest improvement of 4.7-fold (Table 1). A general trend of changing hydrophilic residues into hydrophobic ones was observed in beneficial mutants. The only exception is the Asn to His mutation observed at position 276. The successful selection of single-site libraries of MavCAR on 2-methoxybenzoate in R- Δ 2 host demonstrated that our NADPH recycling-based strategy is viable.

Engineering CAR for Adipate Substrate. To demonstrate its generality, we examined the growth-coupled selection strategy on another unfavorable substrate of MavCAR, adipate. The same experimental protocol as the selection on 2methoxybenzoate was followed. The minimal media selection plate contained adipate at 10 mM, a concentration that is lower than the $K_{\rm m}$ of the wild-type enzyme (Table 2). Colonies with faster growth rate were obtained from six out of the ten libraries (Table S3). Among the 33 clones that were sequenced, at least one mutation was observed multiple times in each of the six libraries (N276, S299, N335, M389, T390, and G391, Table S3). Convergence to a single mutant emerged for positions N335 and M389. The seven mutants with multiple occurrences were characterized (Table 2 and Figure S5). Except for the T390G mutant, which did not have detectable activity, all other mutants showed lower $K_{\rm m}$ toward adipate than that of the wild-type enzyme (62.0 mM). Similar trend of decreasing $K_{\rm m}$ was observed in the 2-methoxybenzoate experiment. Unlike selections on 2-methoxybenzoate, none of the obtained mutants had an improvement in k_{cat} on adipate. Mutant N335R had the lowest $K_{\rm m}$ of 2.6 mM on adipate, which represents an approximately 24-fold improvement (Table 2). It is also the catalytically most active mutant with a 17-fold increase in the catalytic efficiency. We observed that

Table 2. Kinetic Characterization of MavCAR Variants on Adipate a

variants	$K_{\rm m}$ (mM)	$k_{\rm cat}~({\rm min}^{-1})$	$k_{\rm cat}/K_{\rm m}~({\rm min}^{-1}~{\rm mM}^{-1})$
wild-type	62.0 ± 3.9	59.5 ± 1.6	1.0 ± 0.1
N276P (2)	11.1 ± 0.5	47.3 ± 0.5	4.2 ± 0.2
S299K (2)	4.4 ± 0.2	30.1 ± 0.3	6.9 ± 0.3
S299R (4)	13.3 ± 0.8	45.2 ± 0.9	3.4 ± 0.2
N335R (8)	2.6 ± 0.1	44.9 ± 0.6	17.0 ± 1.0
M389K (8)	5.4 ± 0.3	32.3 ± 0.4	5.9 ± 0.4
T390G (2)	Ь	ь	b
G391R (2)	34.2 ± 1.4	29.6 ± 0.3	0.9 ± 0.1
N276R (1)	13.2 ± 0.5	49.3 ± 0.6	3.7 ± 0.2
N335K	9.4 ± 1.3	18.0 ± 0.6	1.9 ± 0.3
M389R	9.7 ± 0.7	33.2 ± 0.8	3.4 ± 0.2

^aNumbers in the parentheses represent the occurrence of mutants. Data are the average of three measurements with standard deviations. ^bThe mutant exhibits no activity.

the introduction of a basic residue, Lys or Arg, in the active site contributes to the large $K_{\rm m}$ decrease in obtained mutants, presumably through engaging in electrostatic interactions with the second carboxylate group of adipate. Again, the exception from this trend was observed at position N276, for which a N276P mutant was detected twice. This mutant showed similar kinetic properties to that of N276R, which contains a mutation into a basic residue (Table 2). It was also observed that each of the two highly converged positions led to a single mutant that contained only one of the two basic amino acid residues (Table 2 and Table S3). To check whether more beneficial mutations were missed in the growth-coupled selection at these sites, mutants N335K and M389R were constructed and characterized (Table 2 and Figure S5). Both mutants did show increased catalytic efficiency, but to a much lower extent in comparison to improvements observed with converged mutants, that is, N335R and M389K (Table 2). While improved mutants were identified, the selection experiment on adipate did lead to two false positives, T390G and G391R, which showed no increase in catalytic efficiency, although both were identified twice.

Aldehydes are versatile intermediates in syntheses. With improved CAR mutants in hand, we further applied them to whole-cell conversions of adipate into a C_6 monomer in the manufacturing of polyester (1,6-hexanediol (1,6-HDO)) through enzymatic reduction of the aldehyde product in CAR-catalyzed reactions (Figure 4A). We first constructed E. coli strains to express an MavCAR variant and an aldehyde reductase (YahK) for the synthesis of 1,6-HDO. The wild-type and five most active CAR mutants were examined (Figure 4B). Cells were cultured in minimal media containing adipate (10

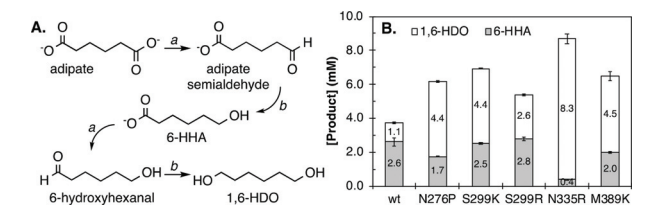


Figure 4. Bioconversions of adipate using MavCAR variants. (A) Reaction schemes: enzymes (a) MavCAR and (b) aldehyde reductase (YahK, *E. coli*). (B) Production of 1,6-HDO and 6-HHA. Data are the average of three cultures with standard deviations.

mM) as the substrate for 24 h. Since MavCARs are active on both adipate and 6-HHA (Figure S6), a mixture of 6-HHA and 1,6-HDO at varied ratios was produced by all strains (Figure 4B). Meanwhile, formation of the two aldehyde intermediates was not detected. Faster conversion was observed when catalytically improved MavCAR mutants were expressed. Meanwhile, the expression level of each CAR variant remained similar (Figure S7). Expression of the best mutant in the adipate selection, N335R, led to the highest combined yield of 6-HHA and 1,6-HDO at 87%. It also afforded the highest ratio between 1,6-HDO and 6-HHA (95:5) as a result of improved kinetics on 6-HHA substrate as well (Figure S6).

Conclusions. In summary, we established a new growthcoupled selection strategy for the engineering of NADPHconsuming enzymes using a genetically modified E. coli host, R- $\Delta 2$. The method was applied to the identification of MavCAR mutants with improved catalytic activities on nonnative substrates, including 2-methoxybenzoate and adipate. Results from the selection of single-site saturated mutagenesis libraries of MavCAR revealed that five residues, N276, M296, S299, N335, and M389, play important roles in the substrate recognition. We also identified N276 as a highly flexible residue. Further insights into the substrate specificity of the mutant enzymes will benefit from structural data. Overall, the NADPH recycling-based growth selection method has a low rate of false positives. In comparison to instrumentintensive mutant screening approaches, our selection method has higher throughput and better accessibility. The method can be further developed for the evolution of other NADPHdependent enzymes. At last, utility of the evolved MavCAR mutants was demonstrated in whole-cell bioconversion of adipate into an industrially important chemical, 1,6-HDO.

METHODS

General methods for media preparation, DNA manipulation, *E. coli* strain construction, growth characterization, protein expression and purification, and metabolite analysis are included in the Supporting Information.

Single-Site Saturation Mutagenesis. To construct single-site saturation mutagenesis libraries, the codon of the target site was randomized using the NNK codon (N = A, C, T, or G, K = T or G, 32 variants at nucleotide level). PCR products covering the randomized sequences were ligated into pZSC101-MavCAR-YahK that was linearized at either the NheI and NsiI sites or two BamHI sites (only for the V423 library). More than 100 clones were obtained for each library, which led to >95% coverage of the library diversity. Quality of the libraries was verified by DNA sequencing.

Growth-Coupled Selection of CAR Mutant Libraries. A single-site library was transformed into chemically competent *E. coli* R-Δ2 that contained the phosphopante-theinyl transferase-expressing plasmid, pZF-Sfp(Ni). Following recovery in LB media, transformants were collected and washed with M9 salts solution. An aliquot that resulted in approximately 100 colony formation units (cfu), was plated on M9 glucose agar plates containing appropriate antibiotics, IPTG (0.25 mM), and a carboxylic acid substrate. Concentrations of the substrate were 1 mM for 2-methoxybenzoic acid and 10 mM for adipic acid, respectively. Every selection experiment also included a transformation plate for the wild-type MavCAR plasmid as the control to gauge growth rates. Colony formation and growth were monitored every 12 h until unambiguous colony formation was observed on the control

plate, which took approximately 72 h. In general, only colonies that appeared before the control strain and had visibly larger size were chosen for further analysis. The number of clones that were further analyzed from each library ranged from 0 to 8, due to varied growth rates. These colonies were introduced into LB media containing ampicillin and cultured for plasmid isolation and DNA sequencing. Plasmids used in the expression of CAR mutants were fully sequenced to confirm there was no additional mutation in the CAR-encoding gene.

Biochemical Assays. All carboxylic acid substrates were purchased either as the free acids or as salts, except for 6hydroxyhexanoic acid (6-HHA), which was obtained by basic hydrolysis of the corresponding commercially available lactone. Kinetic characterization of MavCARs followed a reported protocol. 11 The enzyme assay solution (0.15 mL) contained NADPH (0.15 mM), ATP (1 mM), MgCl₂ (10 mM), glycerol (10%), DTT (1 mM), an appropriate amount of purified protein, and a substrate of interest. Enzyme assays were initiated upon the addition of a substrate of interest. CAR activity was measured spectrophotometrically by monitoring the oxidation of NADPH at 340 nm at 25 °C. A molar extinction coefficient of 6220 M⁻¹ cm⁻¹ (340 nm) was used for NADPH. Blank controls without the carboxylic acid substrate were included for each set of assays. Triplicate experiments were performed for each condition. Kinetic parameters were obtained by analyzing data using Prism 7 (GraphPad Software).

ASSOCIATED CONTENT

Supporting Information

The Supporting Information is available free of charge at https://pubs.acs.org/doi/10.1021/acssynbio.0c00290.

Additional description of methods, list of primers, list of mutations, growth curves, pictures of agar plates, images of SDS-PAGE, and Michaelis—Menten graphs (PDF)

AUTHOR INFORMATION

Corresponding Author

Wei Niu — Department of Chemical & Biomolecular Engineering, University of Nebraska—Lincoln, Lincoln, Nebraska 68588, United States; ⊙ orcid.org/0000-0003-3826-1276; Email: wniu2@unl.edu

Authors

Levi Kramer — Department of Chemical & Biomolecular Engineering, University of Nebraska—Lincoln, Lincoln, Nebraska 68588, United States; orcid.org/0000-0002-1084-4253

Xuan Le — Department of Chemical & Biomolecular Engineering, University of Nebraska—Lincoln, Lincoln, Nebraska 68588, United States

Marisa Rodriguez — Department of Chemical & Biomolecular Engineering, University of Nebraska—Lincoln, Lincoln, Nebraska 68588, United States

Mark A. Wilson — Department of Biochemistry, University of Nebraska—Lincoln, Lincoln, Nebraska 68588, United States; orcid.org/0000-0001-6317-900X

Jiantao Guo — Department of Chemistry, University of Nebraska—Lincoln, Lincoln, Nebraska 68588, United States; orcid.org/0000-0001-6983-9953

Complete contact information is available at: https://pubs.acs.org/10.1021/acssynbio.0c00290

Author Contributions

The manuscript was written through contributions of all authors. All authors have given approval to the final version of the manuscript.

Notes

The authors declare no competing financial interest.

ACKNOWLEDGMENTS

This work was supported by the National Science Foundation, Grant 1805528 to W.N., J.G., and M.A.W. X.L. was supported by the UNL Undergraduate Creative Activities and Research Experience (UCARE) scholarship. M.R. was supported by the Research Experiences for Undergraduates (REU) from National Science Foundation, Grant 1560163.

■ REFERENCES

- (1) He, A., Li, T., Daniels, L., Fotheringham, I., and Rosazza, J. P. N. (2004) *Nocardia* sp. carboxylic acid reductase: cloning, expression, and characterization of a new aldehyde oxidoreductase family. *Appl. Environ. Microbiol.* 70 (3), 1874–1881.
- (2) Venkitasubramanian, P., Daniels, L., and Rosazza, J. P. N. (2007) Reduction of carboxylic acids by *Nocardia* aldehyde oxidoreductase requires a phosphopantetheinylated enzyme. *J. Biol. Chem.* 282 (1), 478–485.
- (3) Venkitasubramanian, P., Daniels, L., and Rosazza, J. P. N. (2007) Biocatalytic reduction of carboxylic acids: mechanism and applications, in *Biocatalysis in the pharmaceutical and biotechnology industries* (Patel, R. N., Ed.), pp 425–440, CRC Press LLC.
- (4) Akhtar, M. K., Turner, N. J., and Jones, P. R. (2013) Carboxylic acid reductase is a versatile enzyme for the conversion of fatty acids into fuels and chemical commodities. *Proc. Natl. Acad. Sci. U. S. A. 110* (1), 87–92.
- (5) Napora-Wijata, K., Robins, K., Osorio-Lozada, A., and Winkler, M. (2014) Whole-cell carboxylate reduction for the synthesis of 3-hydroxytyrosol. *ChemCatChem 6* (4), 1089–1095.
- (6) France, S. P., Hussain, S., Hill, A. M., Hepworth, L. J., Howard, R. M., Mulholland, K. R., Flitsch, S. L., and Turner, N. J. (2016) One-pot cascade synthesis of mono- and disubstituted piperidines and pyrrolidines using carboxylic acid reductase (CAR), *w*-transaminase (*w*-TA), and Imine reductase (IRED) biocatalysts. *ACS Catal.* 6 (6), 3753–3759
- (7) Moura, M., Pertusi, D., Lenzini, S., Bhan, N., Broadbelt, L. J., and Tyo, K. E. J. (2016) Characterizing and predicting carboxylic acid reductase activity for diversifying bioaldehyde production. *Biotechnol. Bioeng.* 113 (5), 944–952.
- (8) Finnigan, W., Thomas, A., Cromar, H., Gough, B., Snajdrova, R., Adams, J. P., Littlechild, J. A., and Harmer, N. J. (2017) Characterization of carboxylic acid reductases as enzymes in the toolbox for synthetic chemistry. *ChemCatChem 9* (6), 1005–1017.
- (9) Khusnutdinova, A. N., Flick, R., Popovic, A., Brown, G., Tchigvintsev, A., Nocek, B., Correia, K., Joo, J. C., Mahadevan, R., and Yakunin, A. F. (2017) Exploring bacterial carboxylate reductases for the reduction of bifunctional carboxylic acids. *Biotechnol. J.* 12 (11), 1600751.
- (10) Stolterfoht, H., Schwendenwein, D., Sensen, C. W., Rudroff, F., and Winkler, M. (2017) Four distinct types of E.C. 1.2.1.30 enzymes can catalyze the reduction of carboxylic acids to aldehydes. *J. Biotechnol.* 257, 222–232.
- (11) Kramer, L., Hankore, E. D., Liu, Y., Liu, K., Jimenez, E., Guo, J., and Niu, W. (2018) Characterization of carboxylic acid reductases for biocatalytic synthesis of industrial chemicals. *ChemBioChem* 19 (13), 1452–1460.
- (12) Kunjapur, A. M., Tarasova, Y., and Prather, K. L. J. (2014) Synthesis and accumulation of aromatic aldehydes in an engineered strain of *Escherichia coli. J. Am. Chem. Soc.* 136 (33), 11644–11654.
- (13) Schwendenwein, D., Fiume, G., Weber, H., Rudroff, F., and Winkler, M. (2016) Selective enzymatic transformation to aldehydes

in vivo by fungal carboxylate reductase from Neurospora crassa. Adv. Synth. Catal. 358 (21), 3414–3421.

- (14) Qu, G., Guo, J., Yang, D., and Sun, Z. (2018) Biocatalysis of carboxylic acid reductases: phylogenesis, catalytic mechanism and potential applications. *Green Chem.* 20 (4), 777–792.
- (15) Winkler, M. (2018) Carboxylic acid reductase enzymes (CARs). Curr. Opin. Chem. Biol. 43, 23-29.
- (16) Derrington, S. R., Turner, N. J., and France, S. P. (2019) Carboxylic acid reductases (CARs): An industrial perspective. *J. Biotechnol.* 304, 78–88.
- (17) Ramsden, J. I., Heath, R. S., Derrington, S. R., Montgomery, S. L., Mangas-Sanchez, J., Mulholland, K. R., and Turner, N. J. (2019) Biocatalytic N-alkylation of amines using either primary alcohols or carboxylic acids via reductive aminase cascades. *J. Am. Chem. Soc.* 141 (3), 1201–1206.
- (18) Gahloth, D., Dunstan, M. S., Quaglia, D., Klumbys, E., Lockhart-Cairns, M. P., Hill, A. M., Derrington, S. R., Scrutton, N. S., Turner, N. J., and Leys, D. (2017) Structures of carboxylic acid reductase reveal domain dynamics underlying catalysis. *Nat. Chem. Biol.* 13 (9), 975–981.
- (19) Gahloth, D., Aleku, G. A., and Leys, D. (2020) Carboxylic acid reductase: Structure and mechanism. *J. Biotechnol.* 307, 107–113.
- (20) Qu, G., Fu, M., Zhao, L., Liu, B., Liu, P., Fan, W., Ma, J.-A., and Sun, Z. (2019) Computational insights into the catalytic mechanism of bacterial carboxylic acid reductase. *J. Chem. Inf. Model.* 59 (2), 832–841.
- (21) Wood, A. J. L., Weise, N. J., Frampton, J. D., Dunstan, M. S., Hollas, M. A., Derrington, S. R., Lloyd, R. C., Quaglia, D., Parmeggiani, F., Leys, D., Turner, N. J., and Flitsch, S. L. (2017) Adenylation activity of carboxylic acid reductases enables the synthesis of amides. *Angew. Chem., Int. Ed.* 56 (46), 14498–14501.
- (22) Kramer, L., Le, X., Hankore, E. D., Wilson, M. A., Guo, J., and Niu, W. (2019) Engineering and characterization of hybrid carboxylic acid reductases. *J. Biotechnol.* 304, 52–56.
- (23) Schwendenwein, D., Ressmann, A. K., Doerr, M., Hoehne, M., Bornscheuer, U. T., Mihovilovic, M. D., Rudroff, F., and Winkler, M. (2019) Random mutagenesis-driven improvement of carboxylate reductase activity using an amino benzamidoxime-mediated high-throughput assay. *Adv. Synth. Catal.* 361 (11), 2544–2549.
- (24) Qu, G., Liu, B., Zhang, K., Jiang, Y., Guo, J., Wang, R., Miao, Y., Zhai, C., and Sun, Z. (2019) Computer-assisted engineering of the catalytic activity of a carboxylic acid reductase. *J. Biotechnol.* 306, 97–104
- (25) Tee, K. L., Xu, J.-H., and Wong, T. S. (2019) Protein engineering for bioreduction of carboxylic acids. *J. Biotechnol.* 303, 53–64.
- (26) Fedorchuk, T. P., Khusnutdinova, A. N., Evdokimova, E., Flick, R., Di Leo, R., Stogios, P., Savchenko, A., and Yakunin, A. F. (2020) One-pot biocatalytic transformation of adipic acid to 6-aminocaproic acid and 1,6-hexamethylenediamine using carboxylic acid reductases and transaminases. *J. Am. Chem. Soc.* 142 (2), 1038–1048.
- (27) Ressmann, A. K., Schwendenwein, D., Leonhartsberger, S., Mihovilovic, M. D., Bornscheuer, U. T., Winkler, M., and Rudroff, F. (2019) Substrate-independent high-throughput assay for the quantification of aldehydes. *Adv. Synth. Catal.* 361 (11), 2538–2543.
- (28) Shen, C. R., Lan, E. I., Dekishima, Y., Baez, A., Cho, K. M., and Liao, J. C. (2011) Driving forces enable high-titer anaerobic 1-butanol synthesis in *Escherichia coli*. *Appl. Environ. Microbiol.* 77 (9), 2905–2915
- (29) Lindner, S. N., Ramirez, L. C., Kruesemann, J. L., Yishai, O., Belkhelfa, S., He, H., Bouzon, M., Doering, V., and Bar-Even, A. (2018) NADPH-auxotrophic *E. coli*: A sensor strain for testing in vivo regeneration of NADPH. *ACS Synth. Biol.* 7 (12), 2742–2749.
- (30) Zhang, L., King, E., Luo, R., and Li, H. (2018) Development of a high-throughput, In vivo selection platform for NADPH-dependent reactions based on redox balance principles. *ACS Synth. Biol.* 7 (7), 1715–1721.
- (31) Martinez, I., Zhu, J., Lin, H., Bennett, G. N., and San, K.-Y. (2008) Replacing *Escherichia coli* NAD-dependent glyceraldehyde 3-

- phosphate dehydrogenase (GAPDH) with a NADP-dependent enzyme from *Clostridium acetobutylicum* facilitates NADPH dependent pathways. *Metab. Eng.* 10 (6), 352–359.
- (32) Machado, H. B., Dekishima, Y., Luo, H., Lan, E. I., and Liao, J. C. (2012) A selection platform for carbon chain elongation using the CoA-dependent pathway to produce linear higher alcohols. *Metab. Eng.* 14 (5), 504–511.
- (33) Wang, Y., San, K.-Y., and Bennett, G. N. (2013) Improvement of NADPH bioavailability in *Escherichia coli* by replacing NAD +-dependent glyceraldehyde-3-phosphate dehydrogenase GapA with NADP+-dependent GapB from *Bacillus subtilis* and addition of NAD kinase. *J. Ind. Microbiol. Biotechnol.* 40 (12), 1449–1460.
- (34) Qiao, K., Wasylenko, T. M., Zhou, K., Xu, P., and Stephanopoulos, G. (2017) Lipid production in *Yarrowia lipolytica* is maximized by engineering cytosolic redox metabolism. *Nat. Biotechnol.* 35 (2), 173–177.
- (35) Canonaco, F., Hess, T. A., Heri, S., Wang, T., Szyperski, T., and Sauer, U. (2001) Metabolic flux response to phosphoglucose isomerase knock-out in *Escherichia coli* and impact of overexpression of the soluble transhydrogenase UdhA. *FEMS Microbiol. Lett.* 204 (2), 247–252.
- (36) Sauer, U., Canonaco, F., Heri, S., Perrenoud, A., and Fischer, E. (2004) The soluble and membrane-bound transhydrogenases UdhA and PntAB have divergent functions in NADPH metabolism of *Escherichia coli. J. Biol. Chem.* 279 (8), 6613–6619.
- (37) Long, C. P., Gonzalez, J. E., Feist, A. M., Palsson, B. O., and Antoniewicz, M. R. (2018) Dissecting the genetic and metabolic mechanisms of adaptation to the knockout of a major metabolic enzyme in *Escherichia coli. Proc. Natl. Acad. Sci. U. S. A. 115* (1), 222–227.
- (38) Yang, J., Yan, R., Roy, A., Xu, D., Poisson, J., and Zhang, Y. (2015) The I-TASSER Suite: protein structure and function prediction. *Nat. Methods* 12 (1), 7–8.
- (39) Trott, O., and Olson, A. J. (2009) AutoDock Vina: Improving the speed and accuracy of docking with a new scoring function, efficient optimization, and multithreading. *J. Comput. Chem.* 31 (2), 455–461.